

<https://doi.org/10.15407/ujpe63.2.121>

M.P. MALOMUZH, V.M. MAKHLAICHUK

I.I. Mechnikov National University of Odesa

(2, Dvoryans'ka Str., Odesa 65026, Ukraine; e-mail: interaktiv@ukr.net)

DIMERIZATION DEGREE OF WATER MOLECULES, THEIR EFFECTIVE POLARIZABILITY, AND HEAT CAPACITY OF SATURATED WATER VAPOR

The properties of water vapor have been studied. The main attention is focused on the physical nature of the effective polarizability of water vapor and the heat capacity of water vapor at a constant volume, with a proper modeling of those parameters being a good test for a correct description of the dimer concentration in various approaches. Thermal vibrations of water dimers are found to be the main factor governing the specific temperature dependences of those characteristics, and the normal coordinates of dimer vibrations are determined. Fluctuations of the dipole moments of dimers and their contribution to the dielectric permittivity of water vapor are considered in detail. The contribution of the interparticle interaction to the heat capacity is taken into account. By analyzing the effective polarizability and the heat capacity, the temperature dependence of the dimer concentration at the vapor-liquid coexistence curve is determined. The noticeable dimerization in saturated water vapor takes place only at temperatures $T/T_c > 0.8$, where T_c is the critical temperature.

Keywords: saturated water vapor, effective polarizability, heat capacity at a constant volume.

1. Introduction

The dimerization of molecules in water vapor has been studied in many works [1–9]. For this purpose, the cited authors used various research methods. In particular, they determine the concentration of dimers c_d in terms of the second virial coefficient [10–12]. They calculated this parameter directly [13–15], which required the knowledge of vibrational and rotational excitation spectra of dimers. Finally, they determined the dimer concentration, by analyzing the thermal conductivity of water vapor. Unfortunately, the corresponding results significantly differ from one another. From whence, it follows that it is the analysis of new properties of water vapor that can help us to choose correct values for c_d . We believe that those properties include such important parameters as the effective polarizability of a molecule and the heat capacity per molecule at a constant volume.

In this connection, we would like to note the following. The effective polarizability of water molecules is

determined by the standard equation

$$\frac{\varepsilon - 1}{\varepsilon + 2} = \frac{4\pi}{3} n_W \alpha_{\text{eff}}, \quad (1)$$

where $n_W = \rho/m_W$ is the concentration of water molecules in vapor, and ρ the density of water vapor. Near the triple point, water vapor is practically not dimerized, and its effective polarizability per molecule is reduced to the quantity

$$\alpha_{\text{eff}} = \alpha_e + \alpha_d, \quad (2)$$

where α_e is the polarizability of the electron shell of a water molecule, and

$$\alpha_d = \frac{\mathbf{d}^2}{3k_B T}$$

is a contribution given by the dipole moment of an isolated water molecule. The analysis of the temperature dependence of α_{eff} for saturated water vapor [15] demonstrates that significant deviations from formula

(2) are observed at $t = T/T_c \geq 0.7$, with the discrepancy growing with the temperature.

It is clear that the general structure of α_{eff} is rather complicated. If the thermal excitations of dimers are neglected, we obtain

$$\alpha_{\text{eff}} = \frac{1}{1 + c_d} [\alpha_e + \alpha_d + c_d(\alpha_e^{(d)} - \alpha_e) + c_d(\alpha_d^{(d)} - \alpha_d)], \quad (3)$$

where $\alpha_e^{(d)}$ and

$$\alpha_d^{(d)} = \frac{\mathbf{d}_d^2}{3k_B T}$$

are the contributions given by the electron shell and the dipole moment of a dimer, respectively, to the effective polarizability. Furthermore, we took into account that the total number of monomers and dimers in water vapor satisfies the equation

$$n_m + n_d = \frac{1}{1 + c_d} \rho / m_W. \quad (4)$$

However, this modification of the effective polarizability only slightly improves the agreement with the experimental results at $t \geq 0.7$. Therefore, a detailed consideration of the role of thermal excitations of molecular dimers in water vapor becomes an important task.

The same difficulties are inherent to the temperature dependence of the heat capacity for water vapor at a constant volume. At $t \leq 0.7$, the heat capacity is described quite satisfactorily by the sum

$$c_V(t) = 6 + c_{\text{int}}(t), \quad (5)$$

where c_{int} is a contribution given by the interaction between monomers (the heat capacity is measured in terms of the Boltzmann constant k_B). However, formula (5) becomes invalid at $t \geq 0.7$, and thermal excitations of dimers have to be taken into account carefully.

The main aim of this work is to study thermal excitations of water dimers and their manifestations in the effective polarizability of water molecules, as well as the heat capacity of water vapor at a constant volume, in detail. Below, we will consider the specific character of normal coordinates for a water dimer, thermally induced variations of the dipole moment of a dimer, the contribution of thermal excitations to the free energy, the generalization of $c_{\text{int}}(t)$ to an

ensemble of monomers and dimers, and their joint effect on the behavior of the effective polarizability of a molecule and the heat capacity of water vapor. We will also compare the temperature dependences of the dimer concentration obtained in works [10–14].

2. Normal Coordinates for Water Dimer Vibrations

Two water molecules have 18 independent degrees of freedom. If those molecules form a dimer, three coordinates are required to describe dimer's center of mass, and three more angular variables are used to describe the rotation of the dimer as a whole. Hence, the vibrational excitations of a dimer have six degrees of freedom.

The choice of normal coordinates for the description of dimer vibrations was discussed in work [16]. Here, we only briefly consider this issue, because we used an obvious form of normal coordinates in our calculations. The axes of the molecular coordinate frame (MCF) are defined as follows (see Fig. 1). The z -axis is directed along the line that passes through the centers of the mass of the molecules, C_1 and C_2 ; and the x -axis lies in the plane formed by the bisectrices of the H–O–H angles in the water molecules in the equilibrium configuration of the dimer. We must take into consideration that vibrations of the dimers do not change the momentum \mathbf{P} of the center of mass and the angular momentum \mathbf{M} of an isolated dimer. In what follows, we put $\mathbf{P} = 0$ and $\mathbf{M} = 0$.

Possible deviations of molecular coordinates from their equilibrium values can be described, by using the following parameters: the distance between the points C_1 and C_2 , the polar angles χ_1 and χ_2 , the azimuthal angles φ_1 and φ_2 , and the rotation angles ϕ_1 and ϕ_2 around the bisectrices. The first normal coordinate is associated with the distance between the centers of the mass of the molecules: $\delta N_1 = \delta r_{C_1 C_2} \equiv \delta r$. In this case, $\delta z_1 = -\frac{1}{2}\delta r$ and $\delta z_2 = \frac{1}{2}\delta r$. The angular variable $\delta N_2 = \delta\varphi$ can play the role of another normal coordinate, if the angles φ_1 and φ_2 are connected with φ by the relations $\delta\varphi_1 = \delta\varphi$ and $\delta\varphi_2 = -\alpha_2\delta\varphi$. The coefficient α_2 is determined from the equation

$$M_z = (I_{zz}^{(1)} - \alpha_2 I_{zz}^{(2)})\delta\varphi = 0$$

and equals $\alpha_2 = I_{zz}^{(1)} / I_{zz}^{(2)}$, where $I_{zz}^{(1)}$ and $I_{zz}^{(2)}$ are the inertial moments of the water molecules with respect

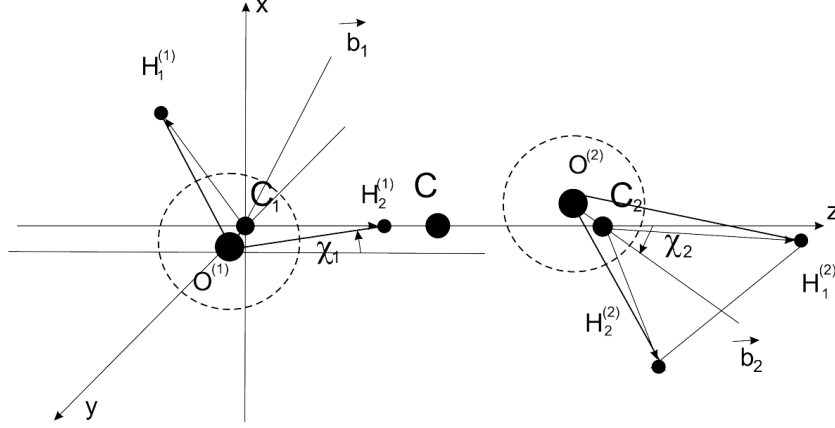


Fig. 1. Water dimer in the molecular coordinate frame: C_1 , C_2 , and C are the centers of mass of the water molecules and the dimer, respectively; $H_1^{(i)}$, $H_2^{(i)}$, and $O^{(i)}$ ($i = 1, 2$) are hydrogen and oxygen atoms; \vec{b}_1 and \vec{b}_2 are bisectrices of the H–O–H angles in the molecules; they are directed along the corresponding dipole moments of the molecules

to the z -axis. The contributions to the kinetic energy written in terms of the indicated normal coordinates read

$$\begin{aligned} T_1 &= \frac{1}{2} m_1 \delta N_1^2, \\ T_2 &= \frac{1}{2} m_2 \delta N_2^2, \end{aligned} \quad (6)$$

where $m_1 = \frac{1}{2} m_w$ and $m_2 = I_{zz}^{(1)} + \alpha_2^2 I_{zz}^{(2)}$.

The third and fourth normal coordinates are associated with the changes of the angles $\delta\chi_1$ and $\delta\chi_2$. Let $\delta M_{y_1}^{(1)} = I_{y_1 y_1}^{(1)} \delta\chi_1$ be an increase of the left molecule momentum. According to the requirement $\mathbf{M} = 0$, this growth must be compensated by the rotation of the right molecule around the y_1 -axis: $\delta M_{y_1}^{(2)} = I_{y_1 y_1}^{(2)} \delta\chi_2 = -\delta M_{y_1}^{(1)}$. Since $I_{y_1 y_1}^{(2)}$ is larger than $I_{y_1 y_1}^{(1)}$ by about an order of magnitude, we may neglect this change. An analogous situation also takes place, when the right molecule rotates. Therefore, those angular variables can be identified with two different normal coordinates: $\delta N_3 \approx \delta\chi_1$ and $\delta N_4 \approx \delta\chi_2$. The corresponding contributions to the kinetic energy are

$$\begin{aligned} T_3 &= \frac{1}{2} m_3 \delta N_3^2, \\ T_4 &= \frac{1}{2} m_4 \delta N_4^2, \end{aligned} \quad (7)$$

where $m_3 = (1 + \alpha_3) I_{y_1 y_1}^{(1)}$, $\alpha_3 = I_{y_1 y_1}^{(1)} / I_{y_1 y_1}^{(2)} < 0.1$, $m_4 = (1 + \alpha_4) I_{y_2 y_2}^{(2)}$, and $\alpha_4 = I_{y_2 y_2}^{(2)} / I_{y_2 y_2}^{(1)} < 0.1$. For

the same reason, the fifth and sixth normal coordinates can be identified with the rotation angles around the bisectrices: $\delta N_5 = \delta\phi_1$ and $\delta N_6 = \delta\phi_2$. In this case,

$$T_5 = \frac{1}{2} m_5 \delta N_5^2, \quad (8)$$

$$T_6 = \frac{1}{2} m_6 \delta N_6^2, \quad (9)$$

where $m_5 = (1 + \alpha_5) I_{b_1 b_1}^{(1)}$, $\alpha_5 = I_{b_1 b_1}^{(1)} / I_{b_1 b_1}^{(2)} < 0.1$, $m_6 = (1 + \alpha_6) I_{b_2 b_2}^{(2)}$, $\alpha_6 = I_{b_2 b_2}^{(2)} / I_{b_2 b_2}^{(1)} < 0.1$.

The expressions for the inertia moments in Eqs. (6)–(9) look like

$$\begin{aligned} I_{zz}^{(1)} &= m r_0^2 (\sin^2(\delta + \chi_1) + \sin^2 \chi_1 - \\ &\quad - \frac{30}{81} \sin(\delta + \chi_1) \sin \chi_1), \end{aligned} \quad (10)$$

$$\begin{aligned} I_{y_1 y_1}^{(1)} &= 2m r_0^2, \quad I_{y_2 y_2}^{(2)} = \frac{144}{81} m r_0^2 \cos^2 \delta / 2, \\ I_{b_1 b_1}^{(1)} &= I_{b_2 b_2}^{(2)} = 2m r_0^2 \sin^2 \delta / 2, \end{aligned} \quad (11)$$

where m is the mass of hydrogen atom, and r_0 the distance between the oxygen and hydrogen atoms in the water molecule. In addition, the following parameter values are used below: $m_w = 18m$, $r_{C_1 C_2} = 2.98 \text{ \AA}$, $r_0 \approx 1/3 r_{C_1 C_2}$, $\chi_1 \approx 2.44^\circ$, $\chi_2 \approx 22.19^\circ$, and $\delta = 109^\circ$ [17]. The coefficients α_i are quoted in Table 1.

3. Mean-Square Fluctuations of the Dipole Moment of Water Dimer

From symmetry reasons, it follows that vibrations of the dipole moment of a water dimer arise, only if the normal coordinates N_2 , N_3 , and N_4 are excited: $\delta N_2 \neq 0$, $\delta N_3 \neq 0$, and $\delta N_4 \neq 0$. So, let us consider all those cases.

The growth of the dimer dipole moment corresponding to the rotation of water molecules around the z -axis equals

$$\delta \mathbf{d}_D = \delta \mathbf{d}_1 + \delta \mathbf{d}_2, \quad (12)$$

where

$$\begin{aligned} \delta \mathbf{d}_1 &= \mathbf{j} d_x \delta \varphi_1 + \dots, \quad \delta \mathbf{d}_2 = \mathbf{j} d_z \delta \varphi_2 + \dots, \\ \delta \varphi_2 &= -\alpha_2 \delta \varphi_1, \end{aligned} \quad (13)$$

and the components \mathbf{d}_1 and \mathbf{d}_2 equal

$$\begin{aligned} \mathbf{d}_1 &= d(\sin(\chi_1 + \delta/2), 0, \cos(\chi_1 + \delta/2)), \\ \mathbf{d}_2 &= d(-\sin \chi_2, 0, \cos \chi_2). \end{aligned}$$

Taking into account that $\delta \varphi_1 \equiv \delta N_2$, we obtain the following result:

$$\begin{aligned} \langle \delta \mathbf{d}_D^2 \rangle_2 &= d^2 A_2(\chi_1, \chi_2) \langle \delta N_2^2 \rangle, \\ A_2(\chi_1, \chi_2) &= (\sin(\chi_1 + \delta/2) + \alpha_2 \sin \chi_2)^2. \end{aligned} \quad (14)$$

Analogously,

$$\langle \delta \mathbf{d}_D^2 \rangle_3 = d^2 A_3(\chi_1, \chi_2) \langle \delta N_3^2 \rangle, \quad (15)$$

$$\begin{aligned} A_3(\chi_1, \chi_2) &= 1 + \alpha_3^2 + 2\alpha_3 \cos(\chi_1 + \chi_2 + \delta/2), \\ \langle \delta \mathbf{d}_D^2 \rangle_4 &= d^2 A_4(\chi_1, \chi_2) \langle \delta N_4^2 \rangle, \end{aligned} \quad (16)$$

$$A_4(\chi_1, \chi_2) = 1 + \alpha_4^2 + 2\alpha_4 \cos(\chi_1 + \chi_2 + \delta/2),$$

where $\alpha_3 = I_{y_1 y_1}^{(1)} / I_{y_1 y_1}^{(2)} \ll 1$ and $\alpha_4 = I_{y_2 y_2}^{(2)} / I_{y_2 y_2}^{(1)} \ll 1$.

Table 1. Dimensionless frequencies, inertia moments, their ratios, and partial contributions to the effective polarizability

Normal coordinates	N_1	N_2	N_3	N_4	N_5	N_6
ω'_k [18]	3.52	2.28	6.97	2.97	10.64	2.71
m'_k		1.449	2.025	0.602	1.326	1.327
α_{N_i}		0.698	0.012	0.004	0.011	0.056
\hat{A}_k		0.048	0.006	0.164		

The increment $\delta \phi_1$ does not change the dipole moment of the left molecule. The compensating rotation of the right molecule changes its dipole moment, but the corresponding modification is negligibly small, and we can omit it. A similar situation also takes place for the increment $\delta \phi_2$.

With a good accuracy, the mean-square values of fluctuations of the normal coordinates N_k ($k = 2, 3, 4$) can be evaluated, by using the classical formula

$$\langle \delta N_k^2 \rangle = \frac{k_B T}{m_k \omega_k^2}, \quad k = 2, 3, 4. \quad (17)$$

Here, $\omega_k^2 = k_{N_k N_k} / m_k$ are the frequencies of normal vibrations ($k = 1 \div 6$), and $k_{N_k N_k}$ are elasticity coefficients. In a more general case, we may write

$$\langle \delta N_k^2 \rangle \approx \frac{k_B T}{m_k \omega_k^2} f(T/T_k),$$

where $T_k = \hbar \omega_k / k_B$. In this formula, the crossover function $f(T/T_k)$ is assumed to be similar to the function that determines the contribution of the k -th vibrational mode to the heat capacity (see Section 7). The behavior of $f(T/T_k)$ for various vibrational modes is shown in Fig. 2.

Let us determine the effective polarizability α_d of a water dimer associated with its vibrations:

$$\alpha_d = \frac{\langle \delta \mathbf{d}_d^2 \rangle}{3k_B T}. \quad (18)$$

In accordance with the aforesaid, we obtain

$$\alpha_d = \alpha_d^{(2)} + \alpha_d^{(3)} + \alpha_d^{(4)}, \quad (19)$$

where

$$\alpha_d^{(k)} = \frac{d^2}{3mr_0^2 \omega_0^2} \frac{A_k(\chi_1, \chi_2)}{m' \omega_k'^2} \quad (k = 2, 3, 4),$$

$m'_k = m_k / (mr_0^2)$, $\omega'_k = \omega_k / \omega_0$, and $\omega_0 = 10^{13} \text{ s}^{-1}$. By the order of magnitude,

$$\frac{d^2}{3mr_0^2 \omega_0^2} \frac{1}{\alpha_e^{(m)}} \approx 10^2,$$

where $\alpha_e^{(m)} \approx 1.05 \times 10^{-24} \text{ cm}^3$ is the electron polarizability of a water monomer. In other words, the effective polarizability of a dimer is substantially higher than its electron polarizability, because $\alpha_e^{(d)} \approx 2\alpha_e^{(m)}$.

Table 2. Ratio $\sqrt{\langle \delta \mathbf{d}_d^2 \rangle} / d_d$ calculated by Eq. (19) for various temperatures

t	0.45	0.5	0.55	0.6	0.65	0.7	0.75	0.8	0.85	0.9	0.95
$\sqrt{\langle \delta \mathbf{d}_d^2 \rangle} / d_d$	0.128	0.134	0.141	0.147	0.153	0.159	0.165	0.170	0.175	0.180	0.185

Numerical values for the partial contributions

$$\tilde{A}_k(\chi_1, \chi_2) = \frac{A_k(\chi_1, \chi_2)}{m'_k \omega_k'^2} \quad (k = 2, 3, 4)$$

to the effective polarizability (19) and for some other parameters are quoted in Table 1. The relative values of fluctuation contributions to the dimer dipole moment at various temperatures are given in Table 2. As one can see, the relative dispersion of the dimer dipole moment does not exceed 8–10% in the whole temperature interval, where the liquid state exists.

4. Dielectric Constant of Dimerized Water Vapor

The dielectric permittivity of dimerized water vapor is determined by the expression [15, 19]

$$\frac{\varepsilon - 1}{\varepsilon + 2} = \frac{4\pi}{3} (n_m + n_d) \left[c_m(t) \left(\alpha_e^{(m)} + \frac{d_m^2}{3k_B T} \right) + c_d(t) \left(\alpha_e^{(d)} + \frac{d_d^2 + \langle \delta \mathbf{d}_d^2 \rangle}{3k_B T} \right) \right],$$

Here,

$$c_m = \frac{n_m}{n_m + n_d}, \quad c_d = \frac{n_d}{n_m + n_d}$$

are the fractions of monomers and dimers, respectively, in water vapor. They satisfy the standard normalization condition

$$c_m + c_d = 1. \quad (20)$$

With the help of Eq. (19), we may write

$$\frac{\varepsilon - 1}{\varepsilon + 2} = \frac{4\pi}{3} (n_m + n_d) \left[c_m \left(\alpha_e^{(m)} + \frac{d_m^2}{3k_B T} \right) + c_d \left(\alpha_e^{(d)} + \alpha_d + \frac{d_d^2}{3k_B T} \right) \right]. \quad (21)$$

Since the sum $n_m + n_d$ is not an experimentally controllable quantity, it has to be related to the density in accordance with Eq. (4). As a result, we obtain

$$\frac{\varepsilon - 1}{\varepsilon + 2} = \frac{4\pi}{3} \frac{\rho}{m_w} \frac{1}{1 + c_d} \left[\alpha_e^{(m)} + \frac{d_m^2}{3k_B T} + \right.$$

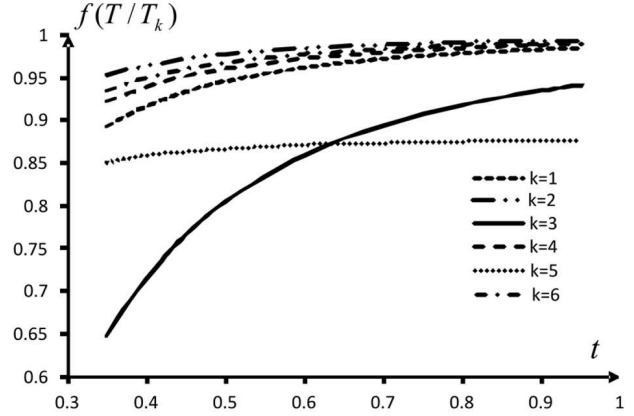


Fig. 2. Temperature dependences of the crossover functions $f(T/T_k)$ for various k

$$+ c_d \left(\alpha_e^{(d)} - \alpha_e^{(m)} + \alpha_d + \frac{d_d^2 - d_M^2}{3k_B T} \right)]. \quad (22)$$

If the dimer concentration is low, formula (22) can be transformed as follows:

$$\frac{\varepsilon - 1}{\varepsilon + 2} \approx \frac{4\pi}{3} \frac{\rho}{m_w} \left[\alpha_e^{(m)} + \frac{d_m^2}{3k_B T} + c_d \left(\alpha_e^{(d)} - 2\alpha_e^{(m)} + \frac{d_D^2 - 2d_m^2}{3k_B T} \right) \right]. \quad (23)$$

5. Analysis of the Dielectric Constant of Saturated Water Vapor

Let us determine the effective polarizability of a water molecule from experimental data obtained for the dielectric constant of saturated water vapor. For this purpose, the formula

$$\alpha_{\text{eff}} = \frac{3}{4\pi} \frac{m_w}{\rho} \frac{\varepsilon - 1}{\varepsilon + 2}$$

is used. The corresponding temperature dependence is shown in Fig. 3.

5.1. Effective polarizability and dimerization degree beyond the critical region

The behavior of the product $\tilde{\alpha}_{\text{eff}} t$ versus the dimensionless temperature $t = T/T_c$, where $\tilde{\alpha}_{\text{eff}} =$

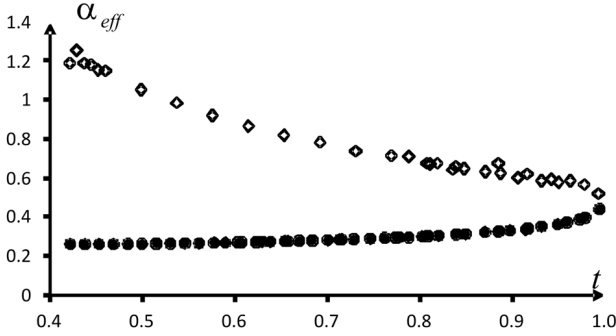


Fig. 3. Temperature dependences of the effective polarizability of a water molecule, α_{eff} , in the saturated vapor (diamonds) and liquid (circles) phases

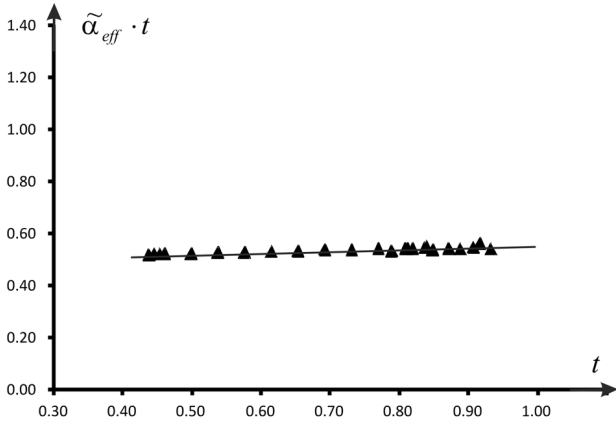


Fig. 4. Experimental temperature dependence of $\tilde{\alpha}_{\text{eff}}$ in the temperature interval $0.43 < t < 0.83$ (triangles). The straight line is its least-squares approximation

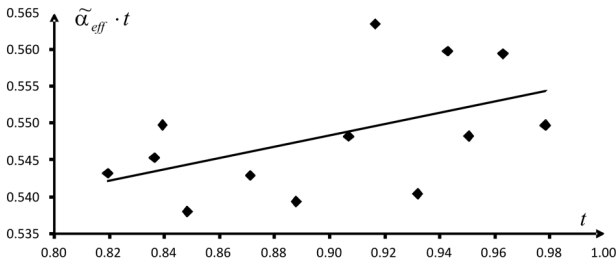


Fig. 5. Dependence of the product $\tilde{\alpha}_{\text{eff}}(t) t$ on the dimensionless temperature t and its linear fitting. Diamonds correspond to experimental data for the dielectric permeability taken from work [21]

$= \alpha_{\text{eff}}/r_{\text{O}_1\text{O}_2}^3$ is the dimensionless effective polarizability, and T_c the critical temperature, is shown in Fig. 4. One can see that the solid curve is practically linear in the temperature interval $0.43 < t < 0.83$; namely, $\tilde{\alpha}_{\text{eff}} t \approx 0.0585t + 0.4845$. The coefficient in

the linear term,

$$\tilde{\alpha}_{\text{eff}} = 0.0585, \quad (24)$$

is close to the polarizability of an isolated water molecule $\tilde{\alpha}_e^{(\text{is})} = 0.055$ [1]. By equating value (24) to the expression

$$\tilde{\alpha}_{\text{eff}}(t) = \tilde{\alpha}_e^{(\text{m})} + c_d(t)(\tilde{\alpha}_e^{(\text{d})} - 2\tilde{\alpha}_e^{(\text{m})} + \tilde{\alpha}_d(t)) + \dots \quad (25)$$

and considering Eq. (23), a conclusion can be made that the concentration of water dimers in saturated water vapor does not exceed 1% in the examined temperature interval. Note that a small difference between $\tilde{\alpha}_{\text{eff}}(t)$ and $\alpha_e^{(\text{is})}$ at $0.43 < t < 0.83$ is naturally explained by two-particle contributions to the effective molecule polarization [15].

The contribution to $\tilde{\alpha}_{\text{eff}}(t)$ that is reciprocal to t has to be attributed to a combination of dipole moments of monomers and dimers:

$$\frac{d_m^2}{3k_B T_c} + c_d(t) \frac{d_D^2 - 2d_m^2}{3k_B T_c} = 13,132 r_{\text{O}_1\text{O}_2}^3.$$

According to work [15], the dipole moment of a dimer equals $d_D^2 = 2d_m^2$. Therefore, we obtain $d_m = 1.87D$, which practically coincides with the experimental value of the dipole moment for a water monomer [1].

Hence, the appreciable dimerization in saturated water vapor is observed only in the temperature interval $0.85 < t < 1$ near the critical point. This conclusion completely agrees with the conclusion of work [20].

5.2. Effective polarizability of a water molecule in a vicinity of the critical point

The values of the product $\tilde{\alpha}_{\text{eff}}(t) t$ in the temperature interval $0.85 < t < 1$ are shown in Fig. 5. Here, the spread of calculation results is significantly larger than that beyond the critical region. Nevertheless, it does not exceed 4%.

The concentration $c_d(t)$ can be evaluated, by using the equation

$$\tilde{\alpha}_{\text{eff}}^{(\text{exc})}(t) = \frac{1}{1 + c_d(t)} \times [\tilde{\alpha}_e^{(\text{m})} + c_d(t)(\tilde{\alpha}_d(t) + \tilde{\alpha}_e^{(\text{d})} - \tilde{\alpha}_e^{(\text{m})})] \quad (26)$$

or

$$\tilde{d}_{\text{eff}}^2 = \frac{1}{1 + c_d(t)} \frac{\tilde{d}_m^2 + c_d(t)(\tilde{d}_d^2 - \tilde{d}_m^2)}{k_B T_c}. \quad (27)$$

Numerical values of $\tilde{\alpha}_{\text{eff}}^{(\text{exc})}(t)$ for a water molecule in various temperature intervals are quoted in the first row of Table 3. The values $\tilde{\alpha}_d = 0.639$ and $\alpha = 0.577$ were calculated in accordance with Eq. ([19]) for different frequency sets taken from work [18] or [16], respectively. In this connection, two values obtained for $c_d(t)$ in accordance with formula (26) are given. Since they are close, we will use the $c_d(t)$ -values calculated, by using the frequency set of work [16]. In effect, those values are averaged over the relevant temperature interval. Those values were used in Eq. (27) to calculate \tilde{d}_{eff}^2 . The experimental and calculated values of \tilde{d}_{eff}^2 are given in the fourth and fifth rows of Table 3. The difference between them is associated with the discrepancy of experimental data for the dielectric permittivity of water vapor, which reaches 4% (see Fig. 5).

It should be noted that the dimer concentrations determined from the analysis of the dielectric permittivity are in satisfactory agreement with the results obtained from the analysis of the temperature dependence $B(T)$ for the second virial coefficient of water vapor (see Table 4) [22]. We also attract attention to that the latter values were determined at a certain temperature, i.e. they were not averaged over the temperature interval. Moreover, our definitions of the dimer concentration c_d and the quantity x_d are connected by the formula

$$c_d(t) = \frac{x_d}{2 - x_d}.$$

5.3. Effective polarizability of a molecule in liquid water

Let us compare the effective polarizabilities of a water molecule when water is in the saturated vapor and liquid states. In the latter case, the behavior of $\tilde{\alpha}_{\text{eff}}(t) t$ is shown in Fig. 6.

In order to interpret the behavior of $\tilde{\alpha}_{\text{eff}}$, let us express the effective polarizability in the form

$$\tilde{\alpha}_{\text{eff}}(t) = \tilde{\alpha}_{\text{eff}}^{(\text{exc})}(t) + \frac{\tilde{d}_{\text{eff}}^2(t)}{3t}, \quad (28)$$

where $\tilde{\alpha}_{\text{eff}}^{(\text{exc})}(t) = \tilde{\alpha}_d(t) + \dots$ is a contribution that arises due to the excitation of cluster vibrations and

$$\tilde{d}_{\text{eff}} = \frac{d_{\text{eff}}(t)}{\sqrt{k_B T_c r_{\text{OO}}^3}}.$$

At the triple point, the effective polarizability of the molecule tends to the value $\tilde{\alpha}_{\text{eff}}^{(\text{exp})} \approx 0.302$, whereas

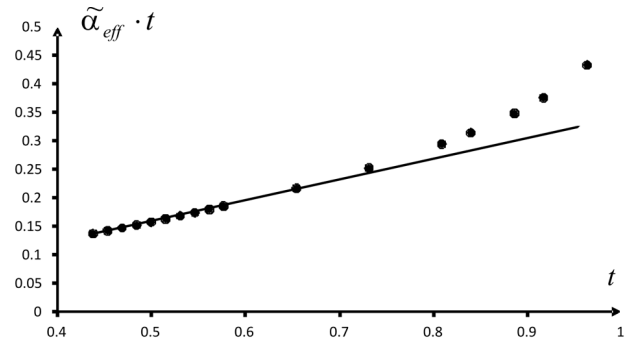


Fig. 6. Temperature dependence of the product $\tilde{\alpha}_{\text{eff}}(t) t$ for liquid water at the coexistence curve in the interval $0.42 < t < 0.91$. Circles correspond to experimental data [21]. The solid line is tangent to the curve $\tilde{\alpha}_{\text{eff}} t$ versus t at the triple point and is described by the equation $\tilde{\alpha}_{\text{eff}} t = 0.302t - 0.02$

$\tilde{d}_{\text{eff}}^{(\text{exp})} \approx 0$. The value of $\tilde{\alpha}_{\text{eff}}^{(\text{exp})}$ corresponds to approximately half the dimensionless effective polarizability of a dimer $\tilde{\alpha}_d(t)$.

Since the effective dipole moment practically vanishes, the following conclusions can be made: 1) the observed value of the effective polarizability per molecule is generated by a set of dimers; 2) two neighbor dimers have antiparallel orientations similar to those in tetramers; and 3) three dimers can form hexamers, similarly to what takes place in hexagonal ice. In all those and similar cases, the dipole moments equal zero. In the liquid state, water dimers are the most stable ones among all mentioned clusters, although all of them are short-lived. Hence, we assume that the dielectric properties of liquid water can be considered as those for an ensemble of

Table 3. Parameters in various temperature intervals

t	0.8–0.98	0.83–0.98	0.85–0.98
$\tilde{\alpha}_{\text{eff}}^{(\text{exc})}(t)$	0.078	0.081	0.126
c_d , [18]	0.045	0.052	0.160
c_d , [16]	0.051	0.060	0.180
\tilde{d}_{eff}^2 (exp)	0.479	0.475	0.433
\tilde{d}_{eff}^2 (calc)	0.493	0.493	0.492

Table 4. $c_d(t)$ -values [22]

t	0.89	0.94	0.968
$c_d(t)$	0.06	0.09	0.14

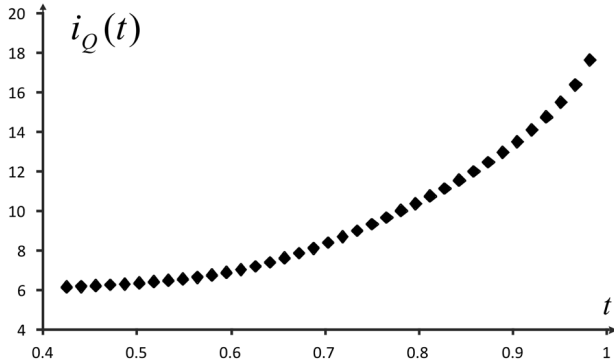


Fig. 7. Temperature dependence of the number of thermal degrees of freedom for saturated water vapor

dimers. The first steps in this direction were made in works [23–26].

Accordingly, we expect that, near the triple point ($t < 0.6$),

$$\alpha_{\text{eff}}^{(\text{exp})} \approx \frac{1}{2} \alpha_d(t). \quad (29)$$

At $t > 0.6$, the situation becomes more complicated. The effective dipole moment per molecule, $d_{\text{eff}}(t)$, now differs from zero. This fact can be naturally explained by the oscillations of the angle between two neighbor dimers that are in antiparallel orientations near the triple point. We intend to consider this issue in a separate paper.

6. Contribution of Attraction Forces to the Heat Capacity of Water Vapor

In this section, the main attention is paid to the temperature dependence of the heat capacity of water vapor. The corresponding experimental dependence [26, 27] is shown in Fig. 7. The heat capacity is expressed in dimensionless units: $i_Q(t) = 2C_V/k_B N_A$. Those units can be interpreted as the number of thermal degrees of freedom per molecule. In a vicinity of the triple point, $i_Q \approx 6$, which corresponds to three translational and three rotational degrees of freedom. As the temperature grows, the following contributions also manifest themselves in the behavior of the heat capacity: the interaction between the particles, dimerization of water molecules, and excitation of dimer vibrations. The dimerization diminishes the number of particles, and i_Q decreases. However, the excitation of dimer vibrations increases the heat capacity. The formation of tetramers and multimers of higher orders leads to further changes in the

heat capacity. Let us consider all those contributions separately.

6.1. Influence of the interaction between molecules on the temperature dependence of the heat capacity

According to work [28], the free energy per molecule in vapor with a relatively high density can be described by the expression

$$f(T, n) = f_{\text{id}} + nTB(T) + \dots,$$

where

$$B(T) = \frac{1}{2} \int (1 - \exp(-\beta U_a(r))) dV, \quad (30)$$

and $U_a(r)$ is an averaged interparticle potential, which is determined by the equation

$$\begin{aligned} \frac{1}{\Omega^2} \int_{\Omega} \int_{\Omega} \exp(-\beta U(r, \Omega_1, \Omega_2)) d\Omega_1 d\Omega_2 &= \\ = \exp(-\beta U_a(r)), \end{aligned} \quad (31)$$

Here, $U(r, \Omega_1, \Omega_2)$ is the “bare” potential of interaction between water molecules (of the SPC or other types), $d\Omega_i$ ($i = 1, 2$) denote unit volumes corresponding to the angular variables, and Ω is the total volume for the angular variables. This definition of averaged potential makes it possible to preserve the value of the configuration integral in the two-particle approximation,

$$\begin{aligned} \frac{1}{\Omega^2} \int_V \int_{\Omega} \int_{\Omega} (1 - \exp(-\beta U(r, \Omega_1, \Omega_2))) d\Omega_1 d\Omega_2 dV &= \\ = \int (1 - \exp(-\beta U_a(r))) dV. \end{aligned}$$

The heat capacity at a constant volume is determined by the standard method. It equals

$$c_v(T) = c_v^{(\text{id})} + c_v^{(\text{int})}, \quad (32)$$

where

$$c_v^{(\text{id})} = 6, \quad (32a)$$

$$c_v^{(\text{int})} = -nT(2B'(T) + TB''(T))|_v. \quad (32b)$$

With the corresponding accuracy, the averaged potential $U_a(r)$ can be approximated by the Lennard-Jones one. Then the heat capacity per molecule at the coexistence curve equals

$$c_v^{(\text{int})}(t) = \frac{2\pi}{3} k_B \tilde{n}_{\text{cc}}(t) (4\tilde{\varepsilon}_a/t)^2 \gamma(\tilde{\varepsilon}_a/t),$$

where

$$\gamma(z) = \int_0^{\inf} \exp(-4z[(1/x)^4 - (1/x)^2]) [(1/x)^4 - (1/x)^2]^2 dx,$$

and the dimensionless variables are defined as follows: $t = T/T_c$, $\tilde{n}_{cc}(t) = n_{cc}(t)\sigma^3$, and $\tilde{\varepsilon}_a = \varepsilon_a/k_B T_c$. The expression for $c_v^{(\text{int})}(\tilde{n}, t)$ is valid as far as the dimer concentration is negligibly low; i.e., at $0.42 < t < 0.83$ [22].

6.2. Influence of the monomer-dimer and dimer-dimer interactions on the temperature dependence of the heat capacity

The free energy of water vapor consisting of monomers and non-excited dimers is determined by the expression

$$f = f_{\text{id}} + T[c_m^2 B_{\text{mm}}(T) + 2c_m c_d B_{\text{md}}(T) + c_d^2 B_{\text{dd}}(T)] + \dots, \quad (33)$$

where

$$B_{ik}(T) = \frac{1}{2} \int (1 - \exp(-\beta U_{ik}^{(a)}(r))) dV \quad (i, k = m, d).$$

All intermediate calculations are similar to those described in the previous section. Hence, the final contribution of the interactions between particles to the heat capacity per molecule looks like

$$c_v^{(\text{int})}(t) = \frac{2\pi}{3} \frac{k_B}{(1+c_d)^2} \frac{\rho_{cc}(t)}{m_w} [(1-c_d)^2 \zeta_m(t) + 2c_d(1-c_d)\zeta_{\text{md}}(t) + c_d^2 \zeta_d(t)],$$

where

$$\zeta_j = \sigma_j^3 (4\tilde{\varepsilon}_j^{(a)}/t)^2 \gamma(\tilde{\varepsilon}_j^{(a)}/t), \quad j = m, \text{md}, d.$$

The “bare” interaction of aqueous monomers was assumed to be described by known potentials of the SPC type. The averaged potentials were calculated by formula (31) and approximated by the Lennard-Jones potential. The corresponding values of its parameters $\tilde{\varepsilon}_m^{(a)}$ and σ_m for water monomers can be found in Table 5.

Note that the screening effects are considered only for the multipole potentials (MP) [29]. The parameters of the Lennard-Jones potential describing the dipole-dipole interaction of two dimers are indicated

in Appendix. The corresponding parameters for the averaged potentials describing the monomer-dimer interaction are defined by the approximate formulas [30]

$$\varepsilon_{\text{md}}^{(a)} = \sqrt{\varepsilon_m^{(a)} \varepsilon_d^{(a)}} \quad \text{и} \quad \sigma_{\text{md}} = \frac{1}{2}(\sigma_m + \sigma_d). \quad (34)$$

The relation

$$\frac{n_m + n_d}{\rho/m_w} = \frac{1}{1 + c_d},$$

which follows from Eq. (4), is also used.

7. Vibrational Contributions to the Heat Capacity

The contribution of vibrations to the free energy of a water dimer is determined by the standard expression [28]

$$F_{\text{vib}} = -T \ln Z_{\text{vib}}, \quad Z_{\text{vib}} = \sum_{k=1}^6 \sum_{n=0}^N \exp(-E_n^{(k)}/T),$$

where

$$E_n^{(k)} = -\varepsilon_0^{(k)} + \hbar\omega_k(n + 1/2),$$

$\varepsilon_0^{(k)}$ is the ground state energy for the k -th mode of dimer vibrations, and N the maximum number of vibrational levels in a finite-depth potential well. Here, we assume that the potential well can be approximated with a satisfactory accuracy by a parabola. The total number of thermal degrees of freedom equals

$$i_Q^{(v)}(t) = \frac{c_d}{1 + c_d} \sum_{k=1}^6 i_q^{(k)}(t), \quad (35)$$

where

$$i_q^{(k)}(t) = 2f(T/T_k), \quad f(T/T_k) = \frac{t_k^2}{t^2} \frac{\exp(t_k/t)}{\exp(t_k/t - 1)^2}, \quad (36)$$

$t_k = T_k/T_c$, and, according to Eq. (4),

$$\frac{n_d}{\rho/m_w} = \frac{c_d}{1 + c_d}.$$

Table 5. σ_m - and $\tilde{\varepsilon}_m^{(a)}$ -values for various averaged “bare” intermolecular potentials

Intermolecular potentials	$\sigma_m, \text{\AA}$	$\tilde{\varepsilon}_m^{(a)}$
SPC	2.62	2.95
TIP3P	2.467	2.792
TIP4P	2.476	2.624
TIP5P	2.458	2.467
MP	2.80	2.187

8. Analysis of Various Contributions to the Heat Capacity of Water Vapor

In this section, the contribution of the monomer-monomer interactions to the number of thermal degrees of freedom for water vapor, corrections due to the monomer-dimer and dimer-dimer interactions, and a contribution by the excitation of dimer vibrations are considered. To compare the calculated values,

$$i_Q(t) = 6 + i_Q^{(mm)} + i_Q^{(md)} + i_Q^{(dd)} + i_Q^{(v)}(t),$$

with experimental data, the values determined for the dimer concentration $c_d(t)$ with the use of the second virial coefficient [12] were used.

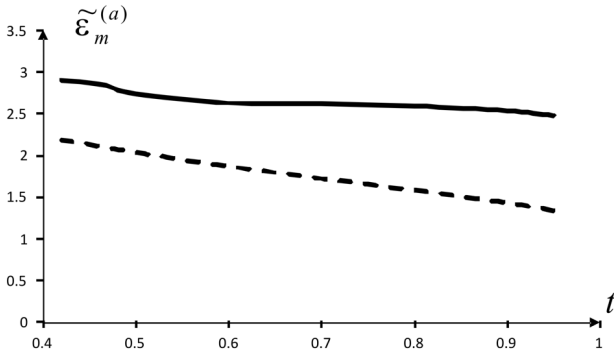


Fig. 8. Temperature dependences of $\tilde{\epsilon}_m^{(a)}$ calculated for the averaged SPC potential (solid curve) and the MP (dashed curve) [29, 31]

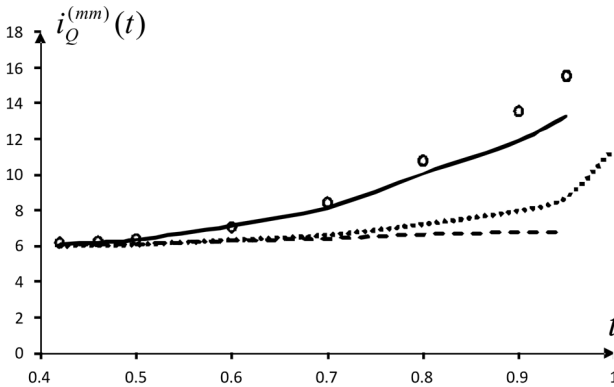


Fig. 9. Temperature dependences of the number of thermal degrees of freedom: (circles) experimental data [27] and calculated (solid curve) for the averaged SPC potential, (dashed curve) for the averaged MP, and (dotted curve), by using the experimental values for the second virial coefficient [32]

8.1. Contribution of the monomer-monomer interaction

Let us start from the expression

$$i_Q(t) = 6 + i_Q^{(mm)}(t) + \dots,$$

where

$$i_Q^{(mm)} \approx \frac{2\pi}{3} \tilde{\rho}_{cc}(t) (4\tilde{\epsilon}_m^{(a)}/t)^2 \gamma(\tilde{\epsilon}_m^{(a)}/t) + \dots,$$

and

$$\tilde{\rho}_{cc}(t) = \frac{\rho_{cc}(t)\sigma_m^3}{m_w}.$$

Attention should be paid that the numerical values of $\tilde{\epsilon}_m^{(a)}(t)$ and $\sigma_m(t)$ calculated in works [22, 29, 31] for the SPC potential depend on the temperature (see Fig. 8), although this effect becomes significant only in a narrow vicinity of the critical point. A comparison of the results obtained for those potentials is exhibited in Fig. 9.

In essence, the behavior of the second virial coefficient is better reproduced with the help of the averaged MP, whereas combination (32b) – this is a combination of the first- and second-order derivatives with respect to the temperature – better reproduces the behavior of heat capacity calculated using the averaged SPC potential. The latter result is accidental, although the effective SPC potential can partially reproduce the contributions $i_Q^{(md)}(t)$ and $i_Q^{(dd)}(t)$ given by the monomer-dimer and dimer-dimer interactions, respectively. They are described by formula (33). In this case, some fine details in the temperature dependences $i_Q^{(md)}(t)$ and $i_Q^{(dd)}(t)$ are associated with the temperature dependence of $\tilde{\epsilon}_m^{(a)}$ depicted in Fig. 8. A significant deviation of the dashed and dotted curves in Fig. 9 from the experimental values clearly testifies to the important role of thermal dimer excitations, because the monomer-dimer and dimer-dimer interactions cannot have a larger influence on the heat capacity than the monomer-monomer interaction has.

8.2. Role of the dimer contributions

In order to reproduce the temperature dependence $i_Q(t)$, we used the values determined for $c_d(t)$ in work [22]. The corresponding results are shown in Fig. 10.

One can see that the experimental data are well reproduced, if $t \leq 0.8$. In this case, the contributions given by the monomer-dimer and dimer-dimer

interactions increase with the temperature and reach about 1%. The contribution of dimer vibrations also increases with the temperature and equals approximately 6%. The application of other $c_d(t)$ -values [9,33,34] results in a worse agreement between the experimental and calculation data. The absence of the complete agreement in the interval $0.8 < t < 0.95$ can be explained by an error in the determination of $c_d(t)$ and the necessity to take trimers and higher-order clusters into consideration [23, 35].

9. Discussion of the Results Obtained

In this work, the physical nature of the polarizability of water molecules in the vapor phase, its effective value per molecule, the heat capacity of water vapor, and the corresponding temperature dependences are considered. If the dimerization and thermal excitations of dimers are taken into account, the behaviors of the effective polarizability and heat capacity are reproduced with a relatively good accuracy. This circumstance is very important indeed, because the experimental data for the heat capacity of water vapor are measured with a high accuracy. From our point of view, the reproduction of the temperature dependences for the effective polarizability and heat capacity of saturated water vapor is one of the best tests for various estimates of $c_d(t)$. The $c_d(t)$ -values were calculated in work [22], by using the experimental data of work [32] for the second virial coefficient. This test allows us to make a conclusion that the results of work [22] are close to optimal ones. Similar results can also be obtained on the basis of experimental data from work [36] (Fig. 11).

It should be emphasized that we did not use the concept of H-bonding. All dimer properties were studied in the framework of electrostatics. In particular, we described the oscillations of the dipole moment of a dimer and its equilibrium parameters. An analogous situation takes place for dimer vibrations. However, this issue was not considered in this paper, because we used the known experimental values for vibration frequencies. We would like to emphasize also that the behaviors of the effective polarizability and heat capacity were also studied in works [23,31]. But, in those works, we used a model based on the vibrations of H-bonds. In that case, the consideration of many details was impossible. At the same time, with an assumption about the electrostatic nature of H-

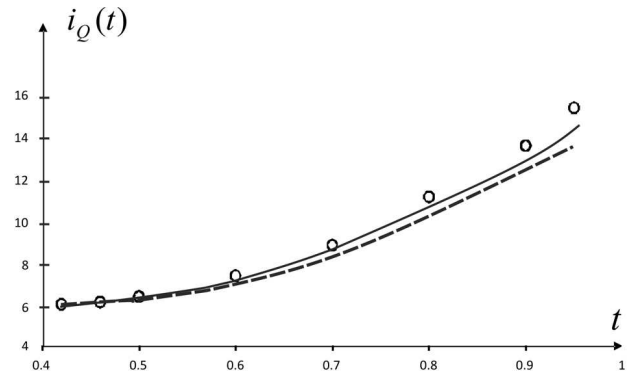


Fig. 10. Temperature dependence $i_Q(t)$ in various approximations: (dashed curve) $i_Q(t) = +i_Q^{(mm)}(t) + i_Q^{(md)}(t) + i_Q^{(dd)}(t)$, (solid curve) $i_Q(t) = +i_Q^{(mm)}(t) + i_Q^{(md)}(t) + i_Q^{(dd)}(t) + i_Q^{(v)}(t)$. Circles correspond to experimental data

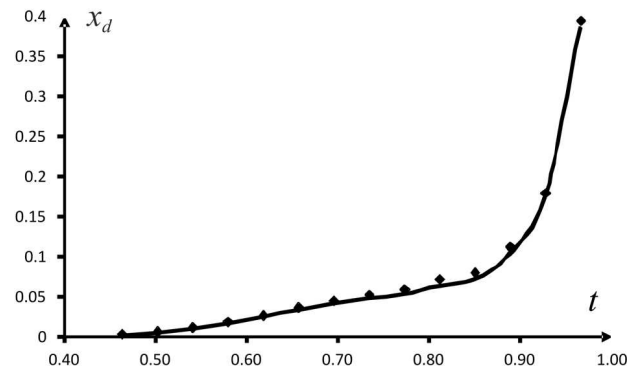


Fig. 11. Temperature dependence of x_d obtained in work [22] making use of experimental data for the second virial coefficient of saturated water vapor [32, 36]

bonds [17, 37–41], those two models become qualitatively equivalent.

Our approach can be generalized to liquid water as well, and this aspect seems to us to be very important. In this case, we are faced with a difficult problem concerning a correct description of clustering in liquid water. However, our assumption that the electrostatic properties of multimers can be simulated, by using a set of dimers makes it possible to draw a satisfactory picture of the liquid water properties. In this approach, an important role belongs to the number of H-bonds per molecule, which are considered to be electrostatic objects. In the framework of an analogous model, the minimum in the heat capacity at a constant pressure, which was observed in works [42, 43] near a temperature of 36°C, is re-

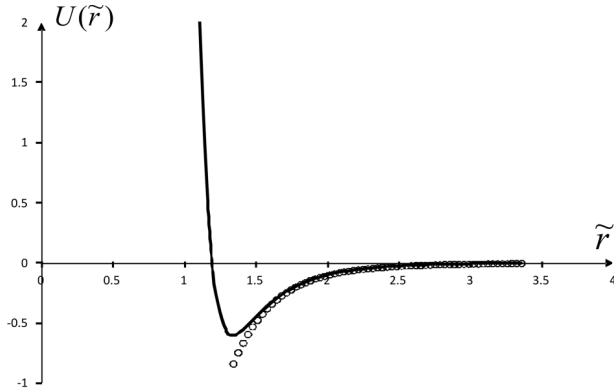


Fig. 12. Comparison between the averaged potential $U_a^{(dd)}(r)$ describing the dipole-dipole interaction between dimers (circles) and the corresponding Lennard-Jones potential (solid curve)

produced quite well. This issue is very important for the physics of living matter, and it will be considered elsewhere.

APPENDIX

Lennard-Jones Potential as an Optimal Approximation for the Behavior of the Averaged Dipole-Dipole Interaction Potential

Let us consider this problem for the potential of dipole-dipole interaction between water dimers. We start from the following definition for the averaged potential $U_a(r)$ (see details and notations in work [44]):

$$\begin{aligned} \exp(-\beta U_a(r)) &= \\ &= \oint_{\Omega_1=4\pi} \frac{d\Omega_1}{4\pi} \oint_{\Omega_2=4\pi} \frac{d\Omega_2}{4\pi} \exp(-\beta\Phi(1,2)). \end{aligned} \quad (37)$$

The numerical values of $U_a(r)$ calculated with the use of formula (37) are shown in Fig. 12 as circles.

In order to determine the parameters $\tilde{\varepsilon} = \varepsilon/k_B T_c$ and $\tilde{\sigma} = \sigma/r_{OO}$ in the corresponding Lennard-Jones potential

$$U_{LJ}(\tilde{r}) = 4\tilde{\varepsilon} \left[\left(\frac{\tilde{\sigma}}{\tilde{r}} \right)^n - \left(\frac{\tilde{\sigma}}{\tilde{r}} \right)^6 \right],$$

where $\tilde{U}_a = U_a/k_B T_c$, let us assume that the numerical values of the product $\tilde{r}^n U_a(\tilde{r})$ are determined by the combination

$$L(\tilde{r}) = -4\tilde{\varepsilon}\tilde{\sigma}^6 \tilde{r}^{n-6} + 4\tilde{\varepsilon}\tilde{\sigma}^n \equiv -a\tilde{r}^{n-6} + b$$

so that they linearly depend on \tilde{r}^{n-6} . Besides that, the optimal n -value corresponds to the case where the values of $\tilde{r}^n U_a(\tilde{r})$ are maximally close to the values of $L(\tilde{r})$ for all \tilde{r} 's.

The parameters $\tilde{\varepsilon}$ and $\tilde{\sigma}$ are related to the parameters a and b by means of the relations $\tilde{\sigma} = (b/a)^{1/(n-6)}$ and $\tilde{\varepsilon} = a^2/(4b)$. One may verify that the optimal n -value for the dipole-dipole interaction equals 12. Then the parameters $\tilde{\varepsilon}$ and $\tilde{\sigma}$ have the following values:

$$\tilde{\varepsilon} = 0.61, \quad \tilde{\sigma} = 1.19.$$

The convergence of the expression to $\tilde{r}^{12} U_a(\tilde{r})$ is illustrated in Fig. 12.

The attention should be paid that, firstly, the value $n = 12$ guarantees that the potentials for water and argon are similar, which results in the argon-like temperature dependences of the specific volume and evaporation heat for water [31]; and, secondly, the parameters $\tilde{\varepsilon}$ and $\tilde{\sigma}$ weakly depend on the temperature.

1. D. Eisenberg, V. Kauzmann. *The Structure and Properties of Water* (Oxford Univ. Press, 1969).
2. K. Burrows, E.R. Pike, J.M. Vaughan. Light-scattering experiments on water vapour at pressures approaching saturation. *Nature* **260**, 131 (1976).
3. G.E. Ashwell, P.A. Eggett, R. Emery, H.A. Gebbie. Molecular complexity of water vapour and the speed of sound. *Nature* **247**, 196 (1974).
4. L. A. Curtiss, D. J. Frurip, M. J. Blander. Studies of molecular association in H₂O and D₂O vapors by measurement of thermal conductivity. *Chem. Phys.* **71**, 2703 (1979).
5. R.A. Bohlander, H.A. Gebbie, G.W.F. Pardoe. Absorption spectrum of water vapor in the region of 23 cm⁻¹ at low temperatures. *Nature* **228**, 156 (1970).
6. J. Hargrove. Water dimer absorption of visible light. *Atmos. Chem. Phys. Discuss.* **7**, 11123 (2007).
7. A.J.L. Shillings, S.M. Ball, M.J. Barber, J. Tennyson, R.L. Jones. An upper limit for water dimer absorption in the 750 nm spectral region and a revised water line list. *Atmos. Chem. Phys.* **11**, 4273 (2011).
8. A.A. Vigasin. Water vapor continuous absorption in various mixtures: possible role of weakly bound complexes. *J. Quant. Spectr. Rad. Transf.* **64**, 25 (2000).
9. A.A. Vigasin, A.I. Pavlyuchko, Y. Jin, S. Ikawa. Density evolution of absorption bandshapes in the water vapor OH-stretching fundamental and overtone: evidence for molecular aggregation. *J. Mol. Str.* **742**, 173 (2005).
10. C.J. Leforestier. Water dimer equilibrium constant calculation: A quantum formulation including metastable states. *Chem. Phys.* **140**, 074106 (2014).
11. J.O. Hirschfelder, F.T. McClure, I.F. Weeks. Second virial coefficients and the forces between complex molecules. *J. Chem. Phys.* **10**, 201 (1942).
12. D. Stogrynt, J.O. Hirschfelder. Contribution of bound, metastable, and free molecules to the second virial coefficient and some properties of double molecules. *J. Chem. Phys.* **31**, 6, 1531 (1959).
13. G. N.I. Clark, D.C. Christopher, J.D. Smith, R.J. Saykally. The structure of ambient water. *Mol. Phys.* **108**, 1415 (2010).
14. Y. Scribano, N. Goldman, R.J. Saykally. Water dimers in the atmosphere III: Equilibrium constant from a flexible potential. *J. Phys. Chem. A* **110**, 5411 (2006).
15. N.P. Malomuzh, V.N. Makhlaichuk, S.V. Hrapatyi. Water dimer dipole moment. *Russ. J. Phys. Chem. A* **88**, 1431 (2014).
16. J.R. Reimers, R.O. Watts. The structure and vibrational spectra of small clusters of water molecules. *Chem. Phys.* **85**, 83 (1984).

17. H.J.C. Berendsen, J.P.M. Postma, W.F. van Gunsteren, J. Hermans. In *Intermolecular Forces*. Edited by B. Pullman (Reidel, 1981).
18. M.J. Smit, G.C. Groenenboom, P.E.S. Wormer, Ad van der Avoird, R. Bukowski, K. Szalewicz. Vibrations, tunneling, and transition dipole moments in the water dimer. *J. Phys. Chem. A* **105**, 6212 (2001).
19. H. Fröhlich. *Theory of Dielectrics: Dielectric Constant and Dielectric Loss* (Clarendon, 1958).
20. V.L. Kulinskii, N.P. Malomuzh. Dipole fluid as a basic model for the equation of state of ionic liquids in the vicinity of their critical point. *Phys. Rev. E* **67**, 011501 (2003).
21. D.P. Fernandez, Y. Mulev, A.R.H. Goodwin, J.M.H. Levelt Sengers. A database for the static dielectric constant of water and steam. *J. Phys. Chem. Ref. Data* **24**, 133 (1995).
22. N.P. Malomuzh, V.N. Makhlaichuk, S.V. Hrapatiy. Water dimer equilibrium constant of saturated vapor. *Russ. J. Phys. Chem. A* **88**, 1287 (2014).
23. N.P. Malomuzh, V.N. Makhlaichuk, P.V. Makhlaichuk, K.N. Pankratov. Cluster structure of water in accordance with the data on dielectric permittivity and heat capacity. *J. Struct. Chem.* **54**, 205 (2013).
24. A.I. Fisenko, N.P. Malomuzh, A.V. Oleynik. To what extent are thermodynamic properties of water argon-like? *Chem. Phys. Lett.* **450**, 297 (2008).
25. L.A. Bulavin, A.I. Fisenko, N.P. Malomuzh. Surprising properties of the kinematic shear viscosity of water. *Chem. Phys. Lett.* **453**, 183 (2008).
26. L.A. Bulavin, T.V. Lokotosh, N.P. Malomuzh. Role of the collective self-diffusion in water and other liquids. *J. Mol. Liq.* **137**, 1 (2008).
27. E.W. Lemmon, M.O. McLinden, D.G. Friend. Thermophysical properties of fluid systems. In *NIST Chemistry WebBook, NIST Standard Reference Database Number 69*. Edited by P.J. Linstrom and W.G. Mallard (National Institute of Standards and Technology, 1999).
28. L.D. Landau, E.M. Lifshitz. *Statistical Physics* (Pergamon, 1980).
29. M.V. Timofeev. Simulation of the interaction potential between water molecules. *Ukr. J. Phys.* **61**, 893 (2016).
30. J.O. Hirschfelder, Ch.F. Curtiss, R.B. Bird. *Molecular Theory of Gases and Liquids* (Wiley, 1954).
31. S.V. Lishchuk, N.P. Malomuzh, P.V. Makhlaichuk. Why thermodynamic properties of normal and heavy water are similar to those of argon-like liquids? *Phys. Lett. A* **374**, 2084 (2010).
32. A.H. Harvey, E.W. Lemmon. Correlation for the second virial coefficient of water. *J. Phys. Chem. Ref. Data* **33**, 369 (2004).
33. G.T. Evans, V. Vaida. Aggregation of water molecules: Atmospheric implications. *J. Chem. Phys.* **113**, 6652 (2000).
34. Y. Scribano, N. Goldman, R.J. Saykally, C. Leforestier. Water dimers in the atmosphere III: Equilibrium constant from a flexible potential. *J. Phys. Chem. A* **110**, 5411 (2006).
35. M.Yu. Tretyakov, D.S. Makarov. Some consequences of high temperature water vapor spectroscopy: Water dimer at equilibrium. *J. Chem. Phys.* **134**, 084306 (2011).
36. Moscow Power Engineering Institute, Mathcad Calculation Server.
37. N.D. Sokolov. Hydrogen bond. *Usp. Fiz. Nauk* **57**, 205 (1955) (in Russian).
38. W.L.J. Jorgensen. Quantum and statistical mechanical studies of liquids. 10. Transferable intermolecular potential functions for water, alcohols, and ethers. Application to liquid water. *Am. Chem. Soc.* **103**, 335 (1981).
39. M.D. Dolgushin, V.M. Pinchuk. Theoretical study of the nature of a hydrogen bond by means of comparative calculations. Preprint ITP-76-49R (Inst. for Theor. Phys. of the NASU, 1976) (in Russian).
40. I.V. Zhyganiuk, M.P. Malomuzh. Physical nature of hydrogen bond. *Ukr. J. Phys.* **60**, 960 (2015).
41. P.V. Makhlaichuk, M.P. Malomuzh, I.V. Zhyganiuk. Potential in the multipole approximation. *Ukr. J. Phys.* **58**, 278 (2013).
42. R.C. Dougherty, L.N. Howard. Equilibrium structural model of liquid water: Evidence from heat capacity, spectra, density, and other properties. *J. Chem. Phys.* **109**, 7379 (1998).
43. *National Institute of Standards and Technology, A gateway to the data collections* [http://webbook.nist.gov].
44. P.V. Makhlaichuk, V.N. Makhlaichuk, N.P. Malomuzh. Nature of the kinematic shear viscosity of low-molecular liquids with averaged potential of Lennard-Jones type. *J. Mol. Liq.* **225**, 577 (2017).

Received 10.08.17.

Translated from Ukrainian by O.I. Voitenko

М.П. Маломуж, В.М. Махлайчук

СТУПІНЬ ДИМЕРИЗАЦІЇ, ЕФЕКТИВНА ПОЛЯРИЗОВАНІСТЬ МОЛЕКУЛ І ТЕПЛОЄМНІСТЬ НАСИЧЕНОЇ ВОДЯНОЇ ПАРИ

Резюме

Робота присвячена дослідженню властивостей водяної пари. Основна увага зосереджена на фізичній природі її ефективної поляризованості та теплоємності при постійному об'ємі. Встановлено, що специфічні температурні залежності цих характеристик зумовлені головним чином тепловими коливаннями димерів води. У зв'язку з цим визначено нормальні координати для коливань димера. Детально досліджені коливання дипольних моментів димерів та розглянуто їх внесок у діелектричну проникність водяної пари. Також враховано внесок міжчастинкової взаємодії до теплоємності водяної пари. Аналізуючи поведінку ефективної поляризованості та теплоємності, визначено температурну залежність концентрації димерів вздовж лінії співіснування рідина-пара. Помітна димеризація в насиченій водяній парі відбувається лише за температури $T/T_c > 0,8$ (де T_c – критична температура). Важливо зазначити, що успішне відтворення ефективної поляризованості та теплоємності може служити хорошим випробуванням для правильного опису концентрації димерів в різних підходах.